STUDY OF FILAMENT WOUND CYLINDERS WITH VAT IN ELASTIC CONDITIONS

Maísa Milanez Ávila Dias Maciel [a], Bruno Cristhoff [a], Sandro Amico [b], Eduardo Gehardt [b], Nuno Viriato Ramos [c], Paulo Tavares [c], Rui Miranda Guedes [c], Volnei Tita [a]

[a]Universitty of São Paulo
Sao Carlos School of Engineering, Brasil, 13563-120
maisa.madm@usp.br, brunogch@gmail.com, voltita@usp.br

[b] Federal University of Rio Grande do Sul
Porto Alegre, Brasil, 90040-060
eduardo.gerhardt.eng@gmail.com, 00146425@ufrgs.br

[c] Porto University, Faculty of Engineering
Porto, Portugal
nviriato@inegi.up.pt, ptavares@inegi.up.pt, rmguedes@fe.up.pt

Keywords: variable angle tow, variable stiffness, VIC 3D, elastic testing, radial compression

1. INTRODUCTION

Carbon fiber reinforced polymers (CFRP) have been widely used not only in secondary structures, but also as primary structures in aircraft [1,2]. On the other hand, the maximum potential of composites is still not utilized, since the only factor considered for composite designs is the high specific strength and stiffness. However, the opportunity to design the structural components considering factors such as anisotropy and the dependence of the fiber architecture on fracture resistance is lost [3].

Traditionally, CFRP are manufactured with an almost isotropic behavior [4]. However, this type of conventional architecture does not fully exploit its anisotropy. Thus, placing the fibers in a continuous and smooth curved path [5–8] can optimize the use of CFRP. These fiber laminates with a curved trajectory are denominated as variable angle tow (VAT), which shows fibers that vary their orientation according to their coordinates in the plane of the lamina [6,9,10].

VAT have shown promising uses in the aeronautical and aerospace industry, due to the increase in resistance to buckling and behavior against vibrations due to their ability to redistribute loads from critical regions to the interior of the laminate [9,11–15]. However, due to the heterogeneous and anisotropic characteristics, different types of occur, leading to very complex mechanical behavior [9]. As the only way to use these materials in primary structures in a safe way is by knowing the initiation and propagation of damage, it becomes essential to study the mechanisms of initiation, propagation, and prediction of damage. VAT present two types of imperfections arising from processing methods, which are resin pockets (gaps) and overlapping reinforcements (overlaps). These imperfections can be hotspots for damage nucleation from mechanical deformations. Within the context of the aeronautical and aerospace industry, this proposal therefore aims to contribute to the development of advanced composite structures without interfering with aircraft safety. The use of VAT laminates can reduce the weight of structures, allowing energy savings for aircraft.

2. METODOLOGY

In this work cylindrical shells of variable stiffness were manufactured by FW using the KUKA KR 140 L100 robot integrated with the MF-Tech control system. The towpreg used is by TCR

composites, in which the filaments are by Toray T700-12K-50C with UF3369 resin system. Unidirectional resistance values were previously obtained and are found in references [21,22]. The cylinders are 130 mm in diameter and the angle variation is 52°/62°(α0)/52° (α1, with two of the three cylinders having a length of 150mm and one of them having a length of 200mm. In addition, they have different winding tension, with 75% and 50%, these variations being in order to reach a more suitable processing condition.

2.1. Radial Compression

The static tests performed is radial compression within the elastic regime with a load ratio of 20 N/min up to a maximum load of 110 N. The test was carried out in two stages, firstly the loading ramp, which presented a pre – load of 0.5 N and ending with 110 N. After the ramp there was a landing where the load is maintained at 110 N for 30 s. The test lasted 6 min in total. The testing was accompanied by digital image correlation 3D due to the materials curvature [23]. The software, Vic3D, performed the acquisition at 45 Hz, but the images were selected later. Spatial resolution was 06 μm/pixel with objective lenses of 60 mm focal length.

2.2. Simulation parameters

The material has 4 layers and approximately 2 mm, and was assumed to have an orientation of 57° (the average between the two maximum angle variations). 3 integration points were used for each layer. At the bottom of the cylinder the following degrees of freedom were restricted u2 = ur1 = ur3 = 0. A displacement of 0.07mm and 0.5mm was applied to the nodes at the top of the cylinder. The value of 0.07 mm is related to 10% of the maximum displacement of the 90° compression test performed on unidirectional samples of the same material. After that, the displacement was increased until a limiting condition given by the Hashin criterion was found. To determine when a material would be 'degraded', the damage initiation model for FRP based on Hashin's theory [24,25] was used, which considers 4 failure modes, fiber traction, fiber compression, traction, and matrix compression, and is already implemented in the ABAQUS distribution. Thus, by using a damage variable, a value of 1.0 or higher indicates that the initiation criterion has been met, so that the propensity of the material to suffer damage can be evaluated without modeling the damage evolution process, considering thus the first ply failure instead of the last ply failure.

3. RESULTS AND DISUSSIONS

It was obtained that the maximum force for 1 mm of displacement was 179 N in the direction of 52°, which would be on the edge of the cylinder, and the maximum value of the Hashin coefficient was in the direction of traction of the matrix and its value was of 0.017. In the tests, the value of 110 N will be used for the maximum load, and the load application rate will be approximately 22 N/min. Figure 1 show the strain map in the 2 (y) direction and the Hashin coefficients map in matrix compression mode, which was the most severe condition found in the simulation. These are the first maps that will be compared with the values obtained by the DIC.

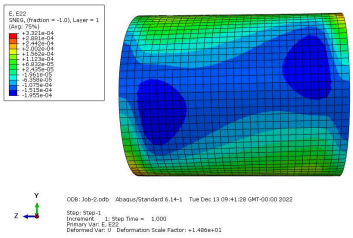

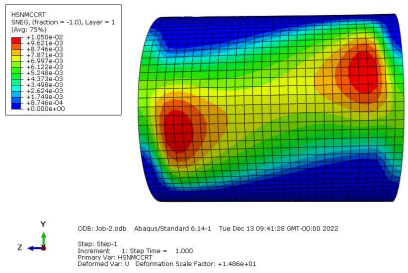

Figure 1. Strain map in direction 2, in side view (y-z plane) and the Hashin coefficients map in compression mode for matrix in side view (y-z plane)

The observed displacements obtained experimentally were close to the one obtained by the simulations for the predicted load in the test. With the 200:75 cylinder having a final displacement of 1.0mm and the 150:50 cylinder having a final displacement of 1.3mm.

Figure 2 shows the final states of deformation in the Y direction, for cylinders 150:50, 150:75 and 200:75, obtained by DIC 3D

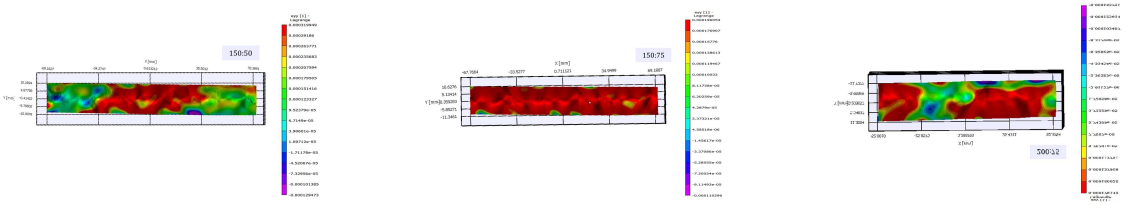

Figure 2 Deformation maps in the Y direction for cylinders 150:50, 150:75 and 200:75

Firstly, it is important to note that only for the 200:75 cylinder, the map only represents half of the cylinder because the length of 200 mm did not allow framing by the lens. At first, there was no correlation between the images, but the observation tracks were made at different points of the cylinder, which may have led to different effects being present in the deformation map, since, according to the literature, the winding pattern of the cylinder can considerably increase the stresses along the length [26]. Furthermore, the literature suggests that winding patterns change stress distributions to non-linear distributions and alter fracture processes of regions [26–28]. It is observed that for cylinder 150:75 the analysis was performed almost to the center of the pattern and for cylinders 150:50 and 200:75 the analysis was displaced from the center of the winding patterns.

4. CONCLUSIONS

Cylinders manufactured with a winding of 52° at the ends and 62° at the center were analyzed in the elastic region by finite elements and with a radial compression test. Simulation analyzes showed a maximum flexion of 1 mm for a load of 110 N which was very close to that obtained for all cylinders 1.0 mm, 1.3 mm and 1.3 mm for cylinders 150:50, 150:75 and 200:75 respectively. The simulation also resulted in a deformation map in the y direction, showing mostly compressive deformations. The experimental radial compression tests, however, show that the cylinders present mainly tensile deformation in the y direction, but that the winding pattern together considerably influences the pattern of the deformation map, which may have affected the results for comparison.

ACKNOWLEDGEMENTS

We would like to acknowledge the founding of FAPESP/FAPERGS and CAPES/FCT number 88887.660187/2021-00. The first author would also like to acknowledge the CAPES PROEX number 88887.817112/2022-00.

REFERENCES

[1] Okabe T. Recent studies on numerical modelling of damage progression in fibre-reinforced plastic composites. Mechanical Engineering Reviews 2015;2:14-00226-14–00226. https://doi.org/10.1299/mer.14-00226.

[2] Djabali A, Toubal L, Zitoune R, Rechak S. An experimental investigation of the mechanical behavior and damage of thick laminated carbon/epoxy composite. *Compos Struct* 2018;184:178–90.
[3] Fanteria D, Lazzeri L, Panettieri E, Mariani U, Rigamonti M. Experimental characterization of the interlaminar fracture toughness of a woven and a unidirectional carbon/epoxy composite — ScienceDirect. *Compos Sci Technol* 2017;142:20–9.
[4] Uhlig K, Tosch M, Bittrich L, Leipprand A, Dey S, Spickenheuer A, et al. Meso-scaled finite element analysis of fiber reinforced plastics made by Tailored Fiber Placement. *Compos Struct* 2016;143:53–62.
[5] Tornabene F, Fantuzzi N, Bacciocchi M. Foam core composite sandwich plates and shells with variable stiffness: Effect of the curvilinear fiber path on the modal response. *Journal of Sandwich Structures and Materials* 2019;21:320–65
[6] Gürdal Z, Tatting BF, Wu CK. Variable stiffness composite panels: Effects of stiffness variation on the in-plane and buckling response. *Compos Part A Appl Sci Manuf* 2008;39:911–22.
[7] Gürdal Z, Olmedo R. In-plane response of laminates with spatially varying fiber orientations: Variable stiffness concept. AIAA/ ASME/ASCE/AHS/ASC 33rd Structures, Structural Dynamics, and Materials Conference, vol. 31, Dallas: 1993, p. 751–8.
[8] Blom AW, Abdalla MM, Gürdal Z. Optimization of course locations in fiber-placed panels for general fiber angle distributions. *Compos Sci Technol* 2010;70:564–70.
[9] Soriano A, Díaz J. Failure analysis of variable stiffness composite plates using continuum damage mechanics models. *Compos Struct* 2018;184:1071–80.
[10] Montemurro M, Catapano A. A general B-Spline surfaces theoretical framework for optimisation of variable angle-tow laminates. *Compos Struct* 2019;209:561–78.
[11] Sousa CS, Camanho PP, Suleman A. Analysis of multistable variable stiffness composite plates. *Compos Struct* 2013;98:34–46.
[12] Almeida JHS, Bittrich L, Jansen E, Tita V, Spickenheuer A. Buckling optimization of composite cylinders for axial compression: A design methodology considering a variable-axial fiber layout. *Compos Struct* 2019;222:110928.
[13] Uhlig K, Bittrich L, Spickenheuer A, Almeida JHS. Waviness and fiber volume content analysis in continuous carbon fiber reinforced plastics made by tailored fiber placement. *Compos Struct* 2019;222:110910.
[14] Yazdani S, Ribeiro P, Rodrigues JD. A p-version layerwise model for large deflection of composite plates with curvilinear fibres. *Compos Struct* 2014;108:181–90.
[15] Yazdani S, Ribeiro P. A layerwise p-version finite element formulation for free vibration analysis of thick composite laminates with curvilinear fibres. *Compos Struct* 2015;120:531–42.
[16] Almeida Júnior JHS, Staudigel C, Caetano GLP, Amico SC. Engineering properties of carbon/epoxy filament wound unidirectional composites. 16th European Conference on Composite Materials, ECCM 2014, Seville: 2014, p. 22–6.
[17] Almeida Júnior JH, Maciel MMÁ dias, Tita V. Effect of Imperfect Fiber/Matrix Interphase: a Micromechanical Model for Predicting Failure in Composite Materials. ABCM International Congress of Mechanical Engineering, Uberlândia: 2019. https://doi.org/10.26678/abcm.cobem2019.cob2019-0623.
[18] Gu Y, Zhang D, Zhang Z, Sun J, Yue S, Li G, et al. Torsion damage mechanisms analysis of two-dimensional braided composite tubes with digital image correction and X-ray micro-computed tomography. *Compos Struct* 2021;256:113020..
[19] Hashin Z. Failure Criteria for Unidirectional FibreComposites. *J Appl Mech* 1980;47:329–34.
[20] Hashin Z, Rotem A. A Fatigue Failure Criterion for Fiber Reinforced Materials. *J Compos Mater* 1973;7:448–64.
[21] Morozov E v. The effect of filament-winding mosaic patterns on the strength of thin-walled composite shells. *Compos Struct* 2006;76:123–9.
[22] Mian HH, Rahman H. Influence of mosaic patterns on the structural integrity of filament wound composite pressure vessels. *International Journal of Structural Integrity* 2011;2:345–56.
[23] Stabla P, Lubecki M, Smolnicki M. The effect of mosaic pattern and winding angle on radially compressed filament-wound CFRP composite tubes. *Compos Struct* 2022;292.

RESPONSIBILITY NOTICE

The author(s) is (are) the only responsible for the printed material included in this manuscript.